Hybrid Block Copolymer Micelles with Partly Hydrophobically Modified Polyelectrolyte Shells in Polar and Aqueous Media: Experimental Study Using Fluorescence Correlation Spectroscopy, Time-Resolved Fluorescence, Light Scattering, and Atomic Force Microscopy†

Pavel Matějíček, Jana Humpolíčková, and Karel Procházka*

Department of Physical and Macromolecular Chemistry and Laboratory of Specialty Polymers, School of Science, Charles University in Prague, Albertov 6, 128 43 Prague 2, Czech Republic

Zdeněk Tuzar and Milena Špírková

Institute of Macromolecular Chemistry, Academy of Sciences of the Czech Republic, Heyrovský Square 2, 162 06 Prague 6, Czech Republic

Martin Hof

The Jaroslav Heyrovský Institute of Physical Chemistry, Academy of Sciences of the Czech Republic, Dolejškova 5, 182 23 Prague 8, Czech Republic

Stephen E. Webber

Department of Chemistry and Biochemistry, University of Texas at Austin, Austin, Texas 78712

Received: October 14, 2002; In Final Form: May 2, 2003

The structure and behavior of amphiphilic block copolymer micelles with partly hydrophobically modified polyelectrolyte shells were studied in 1,4-dioxane−water mixtures and in purely aqueous media by a combination of several experimental techniques. The studied hybrid micelles are formed by 20 wt % of a modified polystyrene-*block*-poly(methacrylic acid), PS-N-PMA-A, double-tagged by one pendant naphthalene between blocks and one anthracene at the end of the PMA block and by 80% of either nontagged PS-PMA or polystyrene-*block*-poly(ethylene oxide), PS-PEO. The cores of micelles contain pure PS, while the shells contain either PMA-A/PMA or PMA-A/PEO mixed chains. The double tagging by naphthalene and anthracene allows for a nonradiative energy transfer (NRET) study aimed at the estimate of donor-trap distances within one micelle. The fluorometric study suggests that the hydrophobic anthracene tag at the end of shell-forming PMA block tries to avoid the aqueous medium and is buried in the shell, forcing the PMA chain to loop back toward the core. Since the stability of hybrid micellar solutions is guaranteed by favorable interactions of stretched unmodified shell-forming chains (which are in excess in the system) with the aqueous solvent, the reduced entropy of the loop-forming chains does not play such an important role as in micelles with 100% tagging. Hence, we conclude that a higher fraction of the anthracene-tagged chains may return closer to the core−corona interface than in the case of 100% tagged micelles.

Introduction

Self-assembled core−shell nanoparticles in aqueous media and various micelle-based amphiphilic nanostructures have been the subject of numerous studies in the past few years.[1−26] Considerable interest of a number of groups in self-assembling water-soluble polymers is motivated by interesting functional properties of prepared nanoparticles and by their potential use in drug and gene delivery.[27−32] Biocompatible self-assembling systems are usually complex, and their behavior is not understood enough to allow for safe biomedical applications. Therefore, studies on relatively simple and well-defined model systems are needed. We have been studying micellization of amphiphilic block copolymers in aqueous and nonaqueous polar media for more than one decade.[33−52] Our long-term research was aimed at understanding basic principles of the micellization behavior and stability of micellar solutions at different conditions because this knowledge is necessary for developing suitable drug delivery systems based on self-assembling polymers.

Amphiphilic block copolymer samples containing a long hydrophobic block, such as polystyrene, PS, and a long polyelectrolyte block, such as poly(methacrylic acid), PMA, are insoluble in aqueous media; nevertheless, multimolecular associates with kinetically frozen PS cores and PMA shells may be prepared indirectly, e.g., by stepwise dialysis.[10] The structure and pH-dependent behavior of the shell is complex and very rich due to the fact that PMA is not only a weak polyelectrolyte,[44,45,53−61] but it has some properties of polysoaps.[62−71]

Recently, we studied micellization of hydrophobically modified block polyelectrolyte copolymers in aqueous media, particularly the behavior of a double-tagged polystyrene-*block*-poly(methacrylic acid) sample, PS-N-PMA-A, tagged by one pendant naphthalene group between blocks and by one an-

† Part of the special issue "International Symposium on Polyelectrolytes".

* To whom correspondence should be addressed. E-mail: prochaz@vivien.natur.cuni.cz.

10.1021/jp022221s CCC: $25.00
Published on Web 06/24/2003

thracene at the end of the PMA block.[49−52] Anthracene and naphthalene form a very suitable pair of fluorophores and have been often used for studies on polymer systems by nonradiative energy transfer.[72−77] In this paper, we report on the behavior of mixed micellar systems formed by (i) modified PS-N-PMA-A and unmodified PS-PMA chains of very similar lengths and composition and (ii) modified PS-N-PMA-A, unmodified PS-PMA, and PS-PEO (poly(ethylene oxide)) chains. Because some authors have been considering the attachment of recognition or modifier groups at the ends of shell-forming blocks in micellar systems for drug and gene delivery, the results of our study may be relevant also for these systems if the recognition groups have some degree of hydrophobicity.[30−32]

Experimental Section

Materials. *Solvents.* 1,4-Dioxane (for fluorescence spectroscopy; Sigma-Aldrich, Int.) was used as purchased. Deionized water and aqueous buffers (analytical grade; Sigma-Aldrich, Int.) were used for all measurements in aqueous media.

Fluorophores. Octadecylrhodamine B (ORB) was purchased from Molecular Probes.

Block Copolymer Samples. Diblock copolymer samples of polystyrene-*block*-poly(methacrylic acid), (i) a single-tagged sample, PS-N-PMA, with one pendant naphthalene tag between blocks, (ii) a double-tagged sample, PS-N-PMA-A, with one pendant naphthalene tag between blocks and one anthracene tag at the end of the poly(methacrylic acid) block, and (iii) *polystyrene*-block-poly(ethylene oxide), PS-PEO were prepared by Dr. C. Ramireddy at the University of Texas using anionic polymerization in tetrahydrofuran at −78 °C in the N_2 atmosphere, as described earlier.[35,37] The structure of copolymers used in our study is depicted in Chart 1. Their molar masses, polydispersity, and composition are given in Table 1.

Techniques. *Dynamic Light Scattering (DLS).* An ALV 5000 multibit, multitau autocorrelator (Langen, Germany) and an He−Ne laser (l_λ = 633 nm) were employed. The solutions for measurements were filtered through 0.22 μm Millipore filters. Measurements were performed with solutions of the lowest possible concentration (ca. 0.1 mg/mL) at different angles and a temperature of 25 °C. Analysis of the data was performed by fitting the experimentally measured $g_2(t)$, the normalized intensity autocorrelation function, which is related to the electrical field correlation function, $g_1(t)$, by the Siegert relation[44,48]

$$g_2(t) - 1 = \beta|g_1(t)|^2 \quad (1)$$

where β is a factor accounting for deviation from ideal correlation. Two different mathematical procedures were used for evaluation of results. (i) For polydisperse samples, $g_1(t)$ can be written as the inverse Laplace transform (ILT) of the relaxation time distribution, $\tau A(\tau)$

$$g_1(t) = \int \tau A(\tau)\exp(-t/\tau)\mathrm{d}\ln\tau \quad (2)$$

where t is the lag-time. The relaxation time distribution, $\tau A(\tau)$, is obtained by performing an inverse Laplace transform (ILT) with the aid of a constrained regularization algorithm (REPES),[78] which minimizes the sum of the squared differences between the experimental and calculated $g_2(t)$. The individual mean diffusion coefficients, D, are calculated from the second moments of the peaks, and the average diffusion coefficient and polydispersity were evaluated using the cumulant method. The hydrodynamic radius R_H was evaluated from the diffusion coefficient using the Stokes−Einstein formula. The viscosity and refractive index of 1,4-dioxane−water mixtures (for evaluation of R_H values) were determined experimentally in our previous studies.[51]

CHART 1: Structures of the Copolymers (a) PS-N-PMA−An, (b) PS-N-PMA, (c)PS-PEO, and (d) PS-PMA

(a)

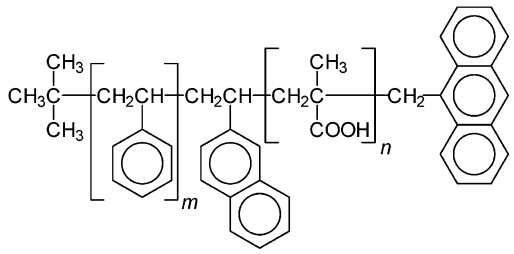

m=300, *n*=340

(b)

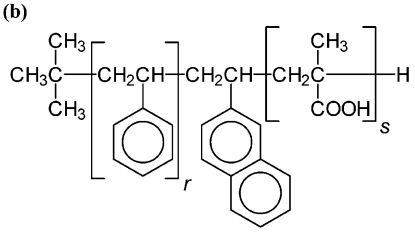

r=220, *s*=365

(c)

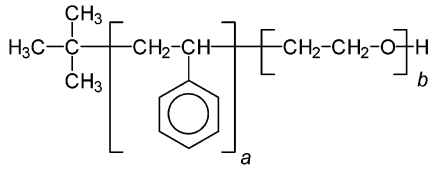

a=190, *b*=435

(d)

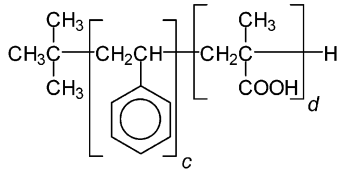

c=275, *d*=155

TABLE 1: Characterization of Polymers[a]

sample	M_w/kg mol^{-1}	x_{PS}	M_w/M_n
PS-PMA	41.6	0.68	1.05
PS-N-PMA-An	60.6	0.52	1.09
PS-N-PMA	54.4	0.42	1.15
PS-PEO	39.0	0.51	1.08

[a] M_w/M_n, determined by size exclusion chromatography. x_{PS} = mass fraction of PS determined by NMR.

Steady-State Fluorometry. Steady-state fluorescence spectra (i.e., corrected excitation and emission spectra and steady-state anisotropy) were recorded with a SPEX Fluorolog 3 fluorometer in a 1 cm quartz cuvette closed with a Teflon stopper. Oxygen was removed by 5 min of bubbling with nitrogen before the measurement.

Time-Resolved Fluorometry. The time-correlated single-photon-counting technique was used for measurements of fluorescence lifetimes. The time-resolved fluorescence decays were recorded on a ED 299 T time-resolved fluorometer, Edinburgh Instruments, Inc., equipped with a nanosecond coaxial discharge lamp filled with hydrogen at 0.5 atm (half-width of the pulse ca. 1.2 ns).[41,43] A reconvolution procedure was used to get the true fluorescence decays that were further

fitted to multiexponential functions using the Marquardt−Levenberg nonlinear least-squares method using the ED software. Low values of χ^2 (close to 1.0) and random distribution of residuals were used as criteria of the fit.

Fluorescence Correlation Spectroscopy. All measurements were performed with a Confocor I apparatus, Carl Zeiss, Jena, Germany, which is a binocular microscope AXIOVERT 135 TV equipped by an adjustable pinhole and a special optics for monitoring fluorescence and a detection diode SPCM-200PQ. An argon laser beam (514 nm) was used for excitation. Autocorrelation curves were obtained using a correlator ALV-5000 (ALV, Langen, Germany) and fitted by means of formulas given below (using a software FCS Access Fit (Evotec, Biosystems, Germany).

Atomic Force Microscopy. All measurements were performed in the tapping mode under ambient conditions using a commercial scanning probe microscope, Digital Instruments Nano-Scope dimensions 3, equipped with a silicon cantilever, Nanosensors, typical spring constant 40 N/m. Polymeric micelles were deposited on a fresh (i.e., freshly peeled out) mica surface (flogopit, ideal formula $KMg_3AlSi_3O_{10}(OH)_2$, Czech Republic, Geological Collection of Charles University in Prague) by a fast dip coating in a dilute micelle solution in pure water (c_P ca. 10^{-3} mg/mL). After the evaporation of water, the samples for AFM were dried in a vacuum oven at ambient temperature for ca. 5 h.

Results and Discussion

Preparation and Characterization of Polymeric Micelles in Solutions by QELS and FCS. The micellization behavior of a 100% double-tagged PS-N-PMA-A and a 100% single-tagged PS-N-PMA was the subject of our previous studies.[49−52] In this paper we study mixed systems as follows: (i) 20 wt % tagged PS-N-PMA-A copolymer and 80% PS-PMA with similar lengths of both blocks and (ii) 20% PS-N-PMA-A and 80% polystyrene-*block*-poly(ethylene oxide), PS-PEO, with a shorter length of the PEO block (see Table 1). The mixed micelles were prepared using the following recipe: single-component micelles were prepared in a 1,4-dioxane (80 vol %)−water (20 vol %) mixed solvent and characterized by QELS. Individual micellar solutions were mixed in the required proportions and stirred for 2 days. In this mild selective solvent a relatively fast exchange of unimer chains between micelles occurs, and since the swollen cores are formed of PS only, the exchange of chains leads to the formation of uniform hybrid micelles.[39,41,46,47] In the case of the PMA-A/PMA shell, the compatibility of both types of chains is obvious. Concerning the micelles with mixed PMA-A/PEO shells, both polymers are fairly compatible and form hydrogen-bond-stabilized interpolymer complexes if PMA is protonated (at low pH).[79−82] Recently, we studied analogous hybrid micelles based on nonmodified PS-PMA and PS-PEO using a combination of various techniques (size-exclusion chromatography, capillary zone electrophoresis, etc.). We found that the full equilibration of the system and formation hybrid micelles is completed in less than 1 day.[47,48] Hybrid micelles were transferred into aqueous buffers by dialysis as described earlier.[34,35] In hybrid aqueous PS-PMA/ PS-N-PMA-A systems, we did not detect any traces of original single-component micelles. In hybrid PS-N-PMA-A/PS-PEO systems, both QELS and AFM data indicate a coexistence of hybrid micelles with a fairly low-weight fraction of single-component PS-PEO micelles (see below).

Hydrodynamic radii, R_H, measured by QELS at different steps of the dialysis are shown in Figure 1 for all micellar systems as a function of the composition of 1,4-dioxane−water solvent. The shape of all curves compares well with our older data for PS-PMA systems.[34,35] Solvents with less than 10 vol % of water are common solvents for PS and PMA, and all studied copolymers dissolve as single chains. In mixtures with 20−50 vol. % of water, reversible multimolecular micelles with swollen PS cores form spontaneously, which is manifested by large hydrodynamic radii. In later dialysis stages the micellization equilibrium freezes, the PS cores de-swell, and hydrodynamic radii, R_H, shrink. In the last dialysis step, the pendant carboxylic groups partially dissociate and the size of micelles increases due to the counterion-mediated (entropy driven) electrostatic repulsion between the charged pendant groups of the shell-forming chains.[45,56,58,59]

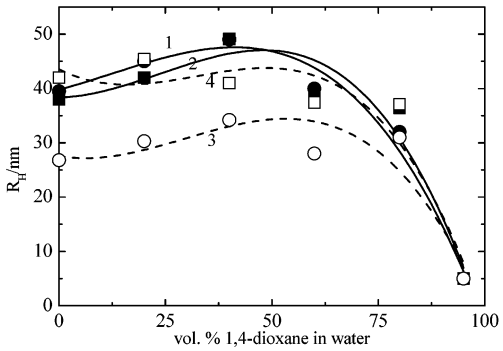

Figure 1. Hydrodynamic radii of polymeric micelles, R_H (in nm), as functions of the composition of the 1,4-dioxane−water solvent. Curves 1 and 2: 20% modified PS-N-PMA/PS-PMA and PS-N-PMA-A/PS-PMA micelles, respectively, curves 3 and 4 hybrid PS-N-PMA/PS-PEO and PS-N-PMA-A micelles, respectively.

Fluorescence Correlation Spectroscopy Study. Fluorescence correlation spectroscopy is not a currently used technique in polymer science. To our knowledge, it was used only by A. Müller et al. for determination of the sizes of polymeric micelles as an auxiliary technique of minor importance in his complex studies,[83,84] although it has frequently been used to study colloidal and biological systems.[85−99] Therefore, we briefly outline the principle advantages and limitations of this technique and explain the determination of the number-average molar masses of micelles by FCS.

FCS is a technique in which temporal fluctuations in the fluorescence measured from a very small volume (ca. 10^{-18} m^3) of a dilute solution (ca. 10^{-9} M) of fluorescent molecules are analyzed to obtain information on processes that give rise to fluorescence fluctuations.[85−87] Under conditions of a typical FCS experiment, the irradiated volume contains only a few fluorophore molecules and each time the fluorescent particle enters or leaves the active volume, a sudden change in the fluorescence intensity is registered. Therefore, we are interested mainly in fluctuations due to translation diffusion in micellar solutions and also by photobleaching as a complicating factor. Time-fluctuating fluorescence intensity measured from a small irradiated volume, $F(t)$, is given by the following formula[87]

$$F(t) = \kappa Q \int W(\mathbf{r},t) C(\mathbf{r},t)\, d\mathbf{r} \qquad (3)$$

where κ is the proportionality constant, Q is the product of absorbtivity, fluorescence quantum yield, and experimental collection efficiency, $C(\mathbf{r},t)$ is the concentration of fluorescent species at position $\mathbf{r}$ in time t, and $W(\mathbf{r},t)$ is a product of the intensity profile of the incident laser beam (usually assumed to be a Gaussian profile) and functions that characterize irradiated volume. The autocorrelation function of fluctuations, which is

used for the evaluation of the diffusion coefficients is given by the following generic equation

$$G(\tau) = 1 + \langle F(t)\cdot F(t+\tau)\rangle / \langle F(t)\rangle^2 \quad (4)$$

where $F(t)$ is the fluorescence intensity in time t and $F(t+\tau)$ is the intensity in time $(t+\tau)$ and the averaging is performed over all measured time interval. If a roughly cylindrical volume of the radius ω_1 and height $2\omega_2$ (corresponding to the focused beam) containing two types of fluorescent particles with the same probabilities of the intersystem crossing, quantum yields ϕ_1 and ϕ_1, and the absorption cross sections σ_1 and σ_1, respectively (typically a probe distributed between two microenvironments), is irradiated by a beam with Gaussian intensity profile, the function $G(t)$ assumes the following form[88]

$$G(\tau) = 1 + \frac{1}{N(1-T)}\{1 - T(1 - e^{-\tau/\tau 0})\} \times \left\{ \frac{1-Y}{1+(\tau/\tau_1)} \frac{(\phi_1\sigma_1)^2}{[1+S^{-2}(\tau/\tau_1)]^{1/2}} + \frac{Y}{1+(\tau/\tau_2)} \frac{(\phi_2\sigma_2)^2}{[1+S^{-2}(\tau/\tau_2)]^{1/2}} \right\} \quad (5)$$

where N is the total number of fluorescent particles in the active irradiated volume, Y and $(1-Y)$ are molar fractions of both species, T is the fraction of molecules converted to the triplet state, τ_0 is the characteristic time for the transition (τ_0^{-1} is the transition rate), S is the ratio of half-axes, $S = \omega_2/\omega_1$, and the irradiated volume $V = 2\pi\omega_1^2\omega_2$. Mathematical treatment of the experimental curve requires a simultaneous fitting of several parameters and is very sensitive and tricky. It was recently the subject of several theoretical papers.[89−93] The diffusion coefficient of the ith component, D_i, may be calculated as $D_i = \omega_1^2/4\tau_i$, and the hydrodynamic radius can be recalculated using the Stokes−Einstein formula, $R_H = kT/(6\pi D\eta)$, where k is Boltzmann's constant, T is the temperature, and η is the viscosity of the solvent.

When using fluorescent probes with a low rate of intersystem crossing and a strong tendency to bind to micelles (e.g., octadecylrhodamine B), the number-average hydrodynamic radius of micelles can be determined. We have found that QELS data for strongly scattering nanoparticles are usually more accurate than FSC data.[100,101] However, hydrodynamic radii obtained by QELS represent mean values recalculated from the z-average diffusion coefficient. They are strongly affected by a low content of larger particles (i.e., larger than the average) but are insensitive to the presence of smaller particles. The FCS values are number averages, weighted evenly by particles of any mass and size. The great advantage of FCS measurements is the possibility of determining the diffusion coefficients of small and only weakly scattering particles or of specifically fluorescent-tagged particles in multicomponent polymer mixtures.

In contrast to the measurement of R_H (for which QELS usually dominates in accuracy), the accuracy of M_n measurements by FCS is fairly high since it is based only on the directly monitored number of scattering particles in the irradiated volume (which is evaluated from the average rate of fluctuations), i.e., it does not require fitting the autocorrelation curve. Further, it is fast, consumes negligible amounts of samples, and does not require a careful filtration (which may be accompanied by the adsorption of a certain amount of micelles on the filter and by uncontrollable changes in polymer concentration). Another considerable advantage of this technique is the fact that it does not require knowledge of the refractive index increment for the studied copolymers. This fact is very important and convenient in complex multicomponent systems, since the value of the refractive index increment obtained under the osmotic equilibrium, $(dn/dc)_\mu$, should be used in mixed solvents for a correct evaluation of experimental data.[102,103] If the preferential sorption of some components is strong and refractive properties of components differ, use of the refractive index increment at constant composition may lead to significant errors. The same applies also for micelles in mixed aqueous solvents and in aqueous buffers containing small ions. The principle of the M_n measurement is the following: Increasing amounts of a fluorescent probe that strongly bind to micelles are added to the measured solution containing a constant concentration of micelles and the particle number (i.e., the average number of fluctuations *per* second) is monitored. For probe-to-micelle ratios lower than 1, the fraction of tagged micelles, i.e., the particle number, increases almost linearly. When all micelles are at least single-tagged, fluorescence fluctuations become larger but their average frequency (particle number) does not change and the curve levels off. From the amount of copolymer and the limiting value of the particle number, the number-average molar mass may be easily calculated.

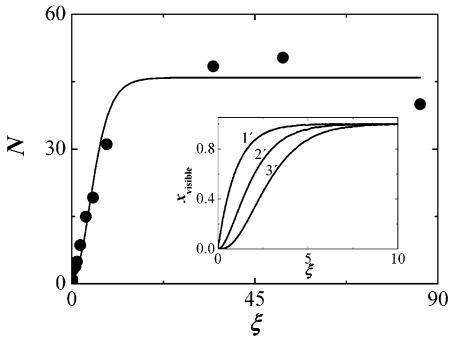

Figure 2. Typical dependence of the particle number, N, on the concentration of the ORB used for the determination of the number-average molar mass of hybrid PS-PMA/PS-N-PMA-A micelles. (Insert) Effects of (i) the Poisson distribution of ORB among polymeric micelles and (ii) the fluorescence quenching on the measured curves.[101] Curve 1' ($x_{visible} = N/N_{max}$ vs ξ): this dependence assumes only the Poisson distribution and no impurity quenching, i.e., each single-tagged micelle is registered. Curve 2': on average only the double-tagged micelles are registered because of the impurity quenching. Curve 3': only the triple-tagged micelles are registered. The leveling-off part of the curve for high ξ yields correct M_n in all cases.

We have shown recently that the M_n determination based on the limiting particle number obtained from the leveling-off part of the curve is not affected by the distribution of probes among individual micelles, not by various quenching processes which are likely to be met under extreme dilutions used for the measurement (unless an important self-quenching occurs at high probe-to-micelle ratios).[101] The accuracy of M_n measurement depends on the determination of the scattering volume (i.e., on the calibration precision) only. A typical dependence of the particle number, N, on the concentration of the fluorescent probe (octadecylrhodamine B) is shown in Figure 2 for mixed PS-PMA/PS-N-PMA-A micelles. The insert in Figure 2 illustrates the role of quenching processes on the particle number for the Poisson distribution of probes in micelles. A brief explanation is given in the pertinent figure caption; a detailed explanation may be found in ref 101. However, theoretical analysis proves unambiguously that N_{lim} obtained from the constant part of the curve for high ξ yields correct M_n values.

TABLE 2: Characterization of Micelles (determined by QELS and FCS (in water))[a]

sample of micelles	M_n/kg mol^{-1}	R_H/nm
PS-N-PMA-An/PS-PMA	1.66×10^3	38.0
PS-N-PMA/PS-PMA	1.09×10^3	39.5
PS-N-PMA-An/PS-PEO	1.12×10^3	42.0
PS-N-PMA/PS-PEO	1.50×10^3	26.8

[a] M_n determined by FCS. R_H determined by QELS.

The number-average molar masses of micelles were measured by fluorescence correlation spectroscopy (FCS) in an alkaline borate buffer (pH ca. 9.2, ionic strength, $I = 0.1$). The weight-average molar masses of the parent PS-N-PMA-A and PS-N-PMA, PS-PEO (SE 5) and PS-PMA (SA 34) micelles were measured in earlier work using static light scattering[50,51] and were compared with FCS data.[100] The M_n values of hybrid micelles obtained by FCS together with R_H values in pure water are given in Table 2. All micelles studied have molar masses larger than 10^6 g/mol.

Study of the Nonradiative Energy Transfer (NRET) by Time-Resolved Fluorometry and the Proposed Structure of PMA/PMA-A and POE/PMA-A Shells in Aqueous Media. In our earlier papers we studied NRET in 100% modified PS-N-PMA-A micelles by steady-sate and time-resolved fluorometry.[49,50] We are using the time-resolved donor (naphthalene) fluorescence decays for evaluation of the energy-transfer efficiency in hybrid systems since they provide reliable data and do not require complicated corrections provided that quenching by impurities is roughly constant in all studied systems. We perform a detailed analysis aimed at distributions of traps in the shell in the accompanying paper devoted to a computer-based simulation study.[100] In this communication we simply fit the NRET-quenched experimental decay, $I_D^q(t)$, by multiexponential functions

$$I_D^q(t) = \sum_i A_i \exp(-\tau_{Fi}/t) \qquad (6)$$

where the sum of preexponential factors A_i is normalized to unity and τ_{Fi} are the lifetime components. By comparing the naphthalene fluorescence decay in PS-N-PMA-A micelles ($I_D^q(t)$) with the reference (nonquenched) decay in PS-N-PMA micelles ($I_D^0(t)$), we are able to draw qualitative conclusions on the behavior of the trap-modifier ends of the shell-forming blocks. The energy-transfer efficiency may be calculated from the relationship

$$\chi_{tr} = 1 - \frac{\langle \tau_F^q \rangle}{\langle \tau_F^0 \rangle} \qquad (7)$$

where $\langle \tau_F^0 \rangle$ and $\langle \tau_F^q \rangle = \sum A_{itFi}$ are linear mean lifetimes of the reference and the modified systems. Typical naphthalene fluorescence decays from PS-N-PMA/ PS-PMA (curve 1) and PS-N-PMA-A/PS-PMA micelles (curve 2) are shown in Figure 3a in a common solvent for both blocks (1,4-dioxane with 5 vol. % water mixture). In this solvent, both samples dissolve as random coils. The average naphthalene−anthracene distance is large, NRET is negligible, and the curves overlap. Analogous curves in water (a strong selective precipitant for PS) are shown in Figure 3b. The NRET quenching at early times is quite pronounced. This result suggests that the anthracene tags try to avoid the aqueous medium and the hydrophobic chain ends loop back toward the core/shell interface.

Energy-transfer efficiency, χ_{tr}, calculated from eq 4, is shown in Figure 4 as a function of the solvent composition. It is evident

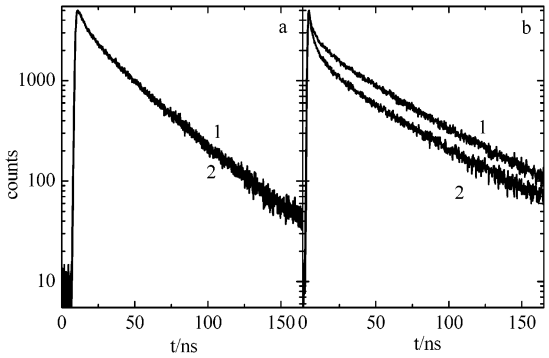

Figure 3. (a) Experimental time-resolved naphthalene fluorescence decays form partially modified PS-N-PMA(20%)/PS-PMA (curve 1) and PS-N-PMA-A(20%)/PS-PMA micelles (curve 2) in a 1,4-dioxane (95 vol %)−water mixture. In this good common solvent for PS and PMA, both curves overlap. (b) The corresponding time-resolved naphthalene fluorescence decays in water which is a strong selective precipitant for PS (curves 1 and 2, same as in part a).

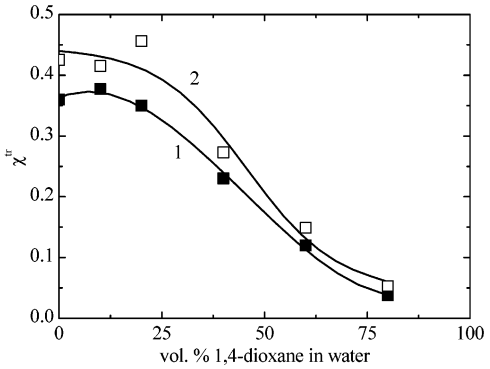

Figure 4. Energy transfer efficiency, χ_{tr} (calculated from the time-resolved fluorescence data), as a function of the 1,4-dioxane−water solvent composition. Curve 1: PS-N-PMA-A (20%)/PS-PMA micelles. Curve 2: PS-N-PMA-A (20%)/PS-PEO micelles.

that NRET is negligible in common solvents and increases with increasing water content. The comparison shows that energy transfer is very efficient even in partially modified systems. Presumably the majority of the NRET in partially modified PS-PMA micelles occurs between N and A that are tethered together on the same polymer chain. The QELS and fluorometry study suggests that the structure and size of hybrid micelles with mixed PMA-A and PMA shells is controlled mainly by the behavior of the majority nonmodified PMA chains (weight fraction is 80%). The modified chains loop back, and since the stability of aqueous micellar solutions is amply secured by the solvation of stretched nonmodified PMA chains with dissociated peripheral COO^- groups, the modified chains loop back even more as compared with the 100% tagged system. Therefore, the measured energy-transfer efficiency, χ_{tr}, is very high (χ_{tr} ca. 0.35 in pure water), taking into account the dilution of both donors and traps in hybrid systems as compared with the fully tagged systems (χ_{tr} ca. 0.25 in pure water).[51]

Concerning PS-N-PMA-A/PS-PEO micelles, we have shown in our earlier papers that the mixed shell has a distinct bilayer structure.[47,48] Dissociation of PMA is suppressed close to the core, and PMA forms a fairly rigid and relatively nonpolar complex with PEO. Since PEO blocks are longer and in excess (weight fraction 80%), parts of PEO chains stretch into the bulk solvent and stabilize the hybrid micelles. Some anthracene traps return close to the core and seem to be trapped in the fairly rigid PMA-PEO complex around the core. This fact is witnessed

not only by strongly quenched naphthalene decays and a fairly high NRET efficiency, but also by very high steady-state anthracene fluorescence anisotropy ($<r>$) of ca. 0.25 in pure water) and almost negligible anthracene fluorescence quenching efficiency, both for the iodide or thallium quenching.

Tapping Mode Atomic Force Microscopy Study and the Structure of Micelles on a Hydrophilic Mica Surface. To further characterize the size distribution of our mixed micelles, we investigated the hybrid micellar systems by atomic force microscopy (AFM). We performed the tapping-mode (TM AFM) studies on micelles deposited on a hydrophilic mica surface by a dip-coating technique. The samples for AFM study were prepared from dilute micellar solutions in pure water in the concentration range $10^{-1}-10^{-3}$ mg/mL. The size and shape of surface-adsorbed micelles are expected to differ from the solution (see ref 101), but we were interested mainly in the relative size distribution to account for differences between the number- and weight-average molar masses found in our recent studies.[101] For hybrid micelles, we were further interested in whether hybridization is complete in mildly selective solvents as the QELS data suggested the possibility of a bimodal distribution of micellar sizes in aqueous PS-N-PMA-A/PS-PEO mixtures.

It is generally recognized that the highly hydrophilic mica surface is negatively charged in aqueous solutions and has often been used for binding polycations.[104−107] Although our PS-PMA micelles are highly charged polyanions, they stick to the fresh mica surfaces. Mica (flogopit-type) is composed of 2D layers of covalently bound aluminum silicate polyanion networks. The layers are kept together by electrostatic forces with small cations (alkaline metals, mainly K^+, and alkaline-earth metals, Mg^{2+}) inserted between the aluminum silicate layers. The freshly peeled off mica surface is covered by metal cations, and its net charge is either neutral or slightly positive. The adhesion of polyanion chains (see below) suggests that during the removal of the thin upper layer, excess cations presumably accumulate on the steady, flat, and atomically smooth lower surface (in comparison with the layer which is deformed during the separation process). The surface cations may be washed out, but our time-dependent pH measurements with grained flogopit particles dispersed in water showed that within the first few seconds only a small fraction of cations is released into the aqueous phase.

The unmodified PS-PMA micelles (SA 34 sample, characterized in refs 43 and 44) and the 100% modified PS-N-PMA-A micelles were studied previously, and the results have been published elsewhere.[50,51] The AFM scans of the mixed micelles demonstrated a low polydispersity of sizes in both cases, although not as low as for the SA 34 PS-PMA single-component micelle. Figure 5a shows a 2.5 μm × 2.5 μm scan of partially modified micelles of PS-N-PMA/PS-N-PMA-A. A 1 μm × 1 μm scan (Figure 5 b) reveals that their average size is ca. 100 nm and compare fairly well with sizes of either PS-PMA or PS-N-PMA-A micelles. However, it is clear from both scans that the polydispersity of mixed micelles is appreciably higher. Figure 5c depicts the corresponding cross-section analysis to show details in the structure of mixed micelles. The maximum vertical distances are almost 25 nm, which compares quite well with the diameter of the rigid (nondeformed) PS core based on the molar mass of micelles and the PS bulk density.[108] The hybrid micelles do not seem to be displaced or deformed during the AFM scan since they keep their round shape and the scans are sharp. The measured profiles show only a small sign of the core/shell structure (almost negligible in comparison with PS-PMA micelles).[100]

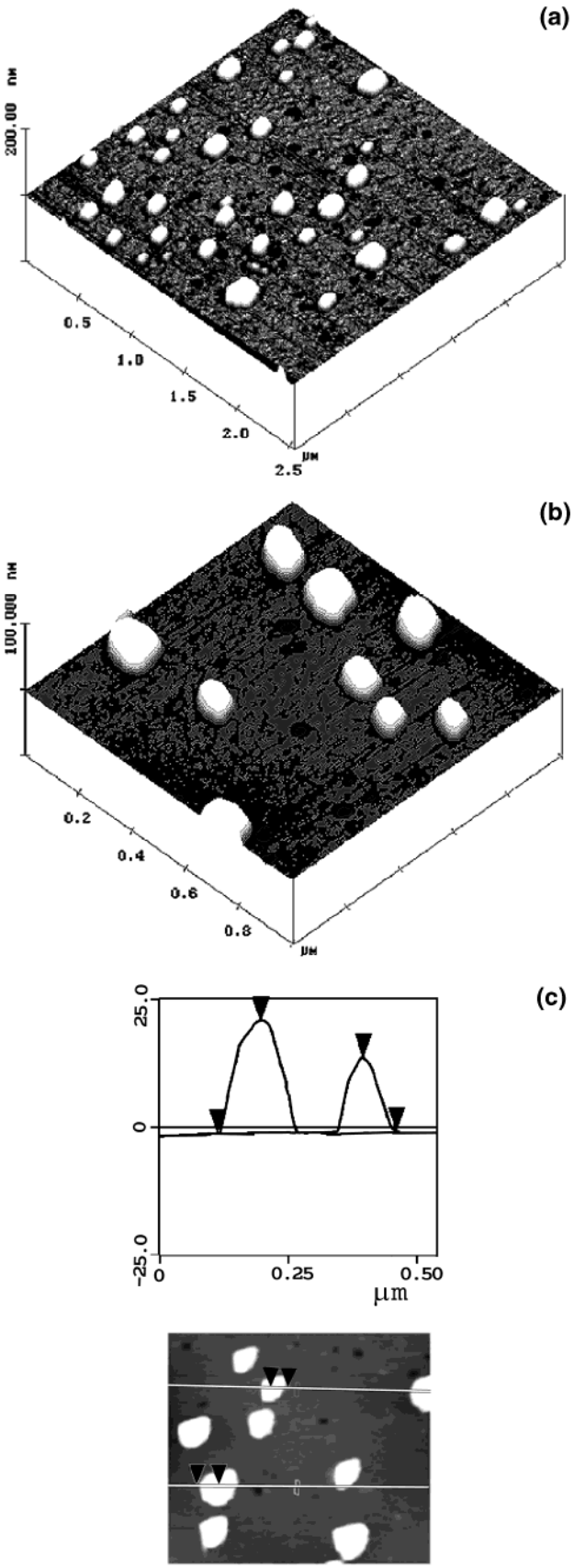

Figure 5. (a) Large tilted 3D (landscape) 2.5 μm × 2.5 μm × 100 nm TM AFM scan of PS-N-PMA-A (20%)/PS-PMA micelles on a mica surface. (b) A detailed 1 μm × 1μm × 100 nm scan of the same system. (c) The corresponding cross-section analysis.

Evaluation of larger scans allows for the determination of histograms of horizontal diameters d and heights h of surface-

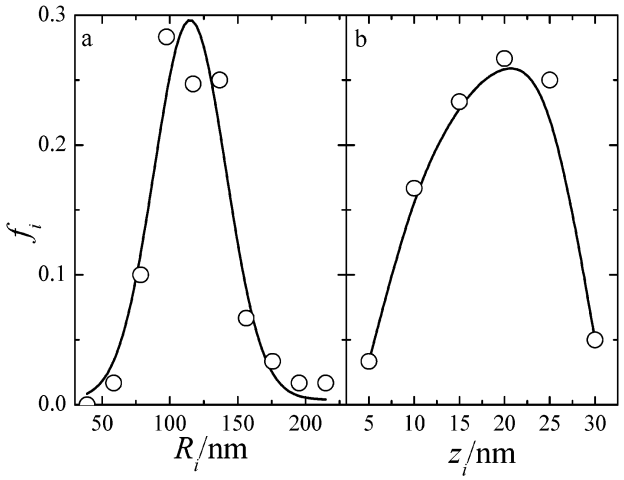

Figure 6. Histogram of micellar sizes evaluated by AFM. (a) Histogram of horizontal radii, R, evaluated on the basis of 300 micelles. (b) Corresponding histogram of heights, z. (c) Cross-correlation of horizontal and vertical values.

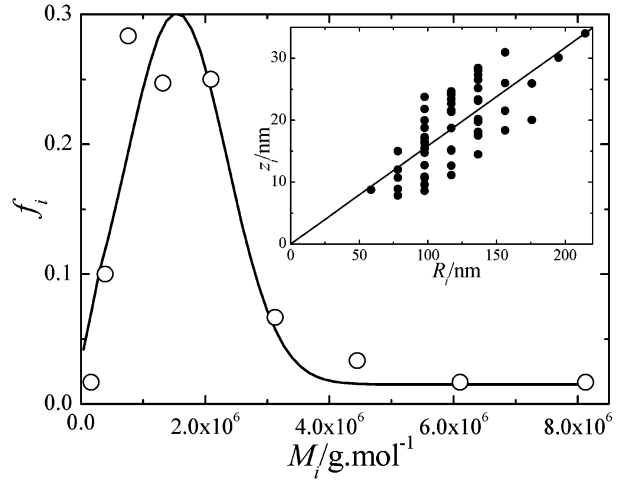

Figure 7. Approximate distribution function of molar masses of hybrid PS-PMA/PS-N-PMA-A micelles based on AFM data. This function was evaluated assuming the proportionality between molar mass, M and the volume of a micelle, i.e., $M \propto R^2z$. Absolute values were obtained by comparing $(M_n)_{exp}$ measured by FCS with the first moment of the distribution. (Insert) Correlation of experimental z_i and R_i values of individual micelles.

deposited micelles and their cross-correlation. The histograms evaluated on the basis of ca. 300 micelles are shown in Figure 6a and b. The cross-correlation of z_i and R_i (based on one scan, i.e., on ca. 60 micelles) is shown in the insert in Figure 7. It clearly proves the linear statistical dependence of z on R (if all points were included, the correlation would be basically identical but too many points would obscure the figure). If we assume that the density of the surface-deposited micelles is spatially constant and that the mass is therefore proportional to the volume (i.e., to the product R^2z), we can estimate the relative distribution of molar masses of mixed micelles. The comparison of the average molar mass, $(M_n)_{rel}$, with experimental value $(M_n)_{exp}$ measured by SCF allows for its recalculation in the absolute distribution function $f_w(M)$. The distribution function obtained by AFM is shown in Figure 7. The weight-average molar mass based on the FCS-estimated $M_n = 1.66 \times 10^3$ kg mol^{-1} and on the AFM-evaluated distribution yields the value $M_w = 2.88 \times 10^3$ kg mol^{-1} and the polydispersity index $M_w/M_n = 1.70$.

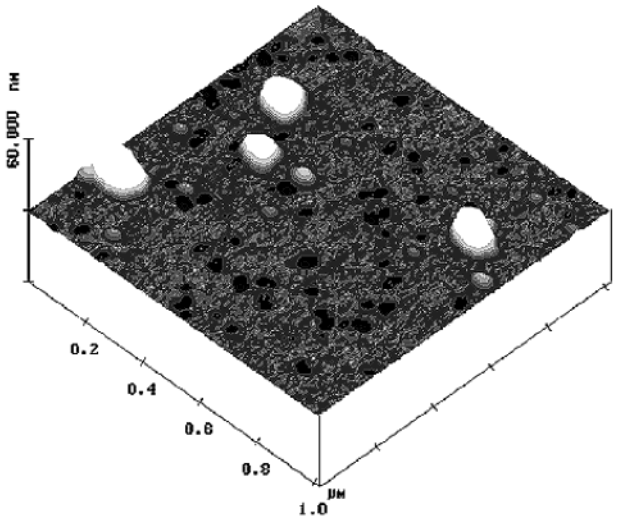

Figure 8. A 1 μm $\times$ 1μm $\times$ 60 nm AFM scan of hybrid PS-N-PMA-A (20%)/PS-PEO micelles on a mica surface. Concentration of the aqueous solution used for the dip coating was ca. 10 times lower than that in previous cases.

In Figure 8, hybrid PS-N-PMA-A/PS-PEO micelles are shown on a 1 μm $\times$ 1 μm scan. In our preliminary AFM studies, we found that micelles with surface-active PEO chains tend to aggregate on the surface. Therefore, we lowered the concentration ca. 10 times as compared with the previous depositions. We succeeded in preventing the aggregation, but the coverage is lower than that in previous figures. The hybrid micelles are fairly monodisperse, but the scan reveals a low-weight fraction of small micelles, which probably are the single-component PS-PEO micelles, since their size is identical with that of the parent PS-PEO micelles (measured independently, but not shown). On the basis of several 5 μm $\times$ 5 μm scans, we can estimate the number ratio of small-to-large micelles as 4/1. Since the radius of the former is ca. 3−4 smaller than that of the latter, we may conclude that the weight fraction of small nonhybridized PS-PEO micelles is less than 10%. This finding is in agreement with QELS results from aqueous solutions of hybrid PS-N-PMA-A/PS-PEO micelles, as the distribution of relaxation times indicated the presence of <10% of smaller particles. Concerning the incomplete hybridization of micelles, supplementary studies are in progress. So far we can offer only a tentative explanation. The PEO blocks are longer than PMA blocks, and therefore, their lower number is needed (as compared with PMA) for the formation of the most convenient complex. Since entropy of mixing favors the presence of several different species and the incorporation of more chains in micelles does not lower the energy any more, two types of micelles−hybrid micelles and single-component PS-PEO micelles are formed.

The AFM study proved that the partially modified PS-N-PMA-A/PS-PMA and hybrid PS-N-PMA-A/PS-PEO micelles are appreciably more polydisperse than the reference PS-PMA micelles (SA34), which may explain differences between molar masses, hydrodynamic radii, and radii of gyration measured by different techniques. When compared with the study for nonmodified PS-PMA and fully modified PS-N-PMA-A micelles,[50,51] it also showed that the hydrophobic modification affects the structure of micelles not only in the solution but also on a hydrophilic surface.

Conclusions

(1) Using a combination of several experimental techniques, we found that the hydrophobically end-tagged PS-N-PMA-A

copolymers form hybrid micelles in aqueous media with PS-PMA and PS-PEO diblocks. These hybrid micelles form spontaneously in a weakly selective solvent (80 vol % dioxane: 20 vol % water) for the PMA or PEO corona.

(2) For both types of hybrid micelles the stability of micellar solutions is provided by the favorable interactions of the stretched nonmodified chains with the solvent. The behavior of the PMA-A chains differs from that of nontagged chains because the anthracene tags tend to be located in the relatively hydrophobic inner shell close to the PS core. Thus, the modified chains are forced to loop back toward the core. Since both the enthalpy and entropy of the system are controlled mostly by the behavior of nonmodified PMA shell-forming blocks, which are in a great excess in our hybrid systems, the decrease in entropy due to the formation of PMA-A chain loops is not as disfavored as in a micelle composed solely of PS-N-PMA-A[51] and the extent of NRET in hybrid micelles is even higher than that in the 100% tagged systems.

(3) The present study provides insights that may be useful in the design of drug and gene delivery systems based on self-assembly of copolymers. Some authors have been considering the attachment of recognition or regulator groups at the ends of shell-forming blocks.[30−32] If these recognition groups have a significant degree of hydrophobicity, then they may also bury themselves in the inner corona region and be inaccessible.

(4) AFM was used for (i) characterization of the distribution in micellar sizes and (ii) study of the behavior of different micelles at the hydrophilic mica surface.

(5) We found that FCS using octadecylrhodamine B as a fluorescent probe is a suitable and fast technique for the characterization of polymer micelles, simultaneously determining the hydrodynamic radii and the number average molar masses.

Acknowledgment. The study is a part of the long-term Research Plan of the School of Science of the Charles University in Prague No. MSM 113100001. This study was supported by the Grant Agency of the Czech Republic (K.P. and Z.T: Grant No. 203/01/0536, M.Š: Grant No. 203/01/0735) and by the Grant Agency of the Charles University in Prague (K.P. Grant No. 215/2000/BCh/Pr). M.H. would like to acknowledge the support of the Ministry of Education of the Czech Republic (LN 00A032) and S.E.W. the support from the Robert Welch Foundation (Grant F-356).

References and Notes

(1) Riess, G.; Hurtres, G.; Bahadur, P. In *Encyclopedia of Polymer Science and Engineering*, 2nd ed.; Wiley: New York, 1985; p 234.

(2) Tuzar, Z.; Kratochvíl, P. In *Surface and Colloid Science*; Matijevic, E., Ed.; Plenum Press: New York, 1993; Vol. 15, p 1.

(3) Almgren, M.; Brown, W.; Hvidt, S. *Colloid Polym. Sci.* **1995**, *273*, 2.

(4) Khougaz, K.; Astafieva, I.; Eisenberg, A. *Macromolecules* **1995**, *28*, 7135.

(5) Tuzar, Z. In *Solvents and Self-organization of Polymers*; Webber, S. E., Munk, P., Tuzar, Z., Eds.; NATO ASI Series E; Kluwer Academic Publishers: Dordrecht 1996; Vol. 327, p 309.

(6) Tuzar, Z.; Pospíšil, H.; Pleštil, J.; Lowe, A. B.; Baines, L. B.; Billingham, N. C.; Armes, S. P. *Macromolecules* **1997**, *30*, 2509.

(7) Tsisilianis, C.; Voulgaris, D.; Štěpánek, M.; Podhájecká, K.; Procházka, K.; Tuzar, Z.; Brown, W. *Langmuir* **2000**, *16*, 6868.

(8) Procházka, K.; Martin, T. J.; Webber, S. E.; Munk, P. *Macromolecules* **1996**, *29*, 6526.

(9) Tuzar, Z. In *Solvents and Self-organization of Polymers*; Webber, S. E., Munk, P., Tuzar, Z., Eds.; NATO ASI Series E; Kluwer Academic Publishers: Dordrecht, 1996; Vol. 327, p 327.

(10) Tuzar, Z.; Webber, S. E.; Ramireddy, C.; Munk, P. *Polym. Prepr.* **1991**, *32* (1), 525.

(11) Munk, P. In *Solvents and Self-organization of Polymers*; Webber, S. E., Munk, P., Tuzar, Z., Eds.; NATO ASI Series E; Kluwer Academic Publishers: Dordrecht, 1996; Vol. 327, p 19.

(12) Wilhelm, M.; Zhao, C.-L.; Wang, Y.; Xu, R.; Winnik, M. A.; Mura, J.-L.; Riess, G.; Croucher, M. D. *Macromolecules* **1991**, *24*, 1033.

(13) Rager, T.; Meyer, W. H.; Wegner, G.; Winnik, M. A. *Macromolecules* **1997**, *30*, 4911.

(14) Astafieva, I.; Zhong, X. F.; Eisenberg, A. *Macromolecules* **1993**, *26*, 7339.

(15) Astafieva, I.; Khougaz, K.; Eisenberg, A. *Macromolecules* **1995**, *28*, 7127.

(16) Yu, Y. S.; Zhang, L. F.; Eisenberg, A. *Langmuir* **1997**, *13*, 2578.

(17) Zhang, L. F.; Eisenberg, A. *Macromolecules* **1999**, *32*, 2239.

(18) Shen, H. W.; Zhang, L. F.; Eisenberg, A. *J. Am. Chem. Soc.* **1999**, *121*, 2728.

(19) Shen, H. W.; Eisenberg, A. *J. Phys. Chem. B* **1999**, *103*, 9473.

(20) Shen, W. H.; Eisenberg, A. *Macromolecules* **2000**, *33*, 2561.

(21) Antonietti, M.; Heinz, S.; Schmidt, M.; Rosenauer, C. *Macromolecules* **1994**, *27*, 3276.

(22) Antonietti, M.; Förster, S.; Östrich, S. *Macromol. Symp.* **1997**, *121*, 75.

(23) Regenbrecht, M.; Akari, S.; Förster, S.; Mohwald, H. *J. Phys. Chem. B* **1999**, *103*, 6669.

(24) Buthun, V.; Lowe, A. B.; Billingham, N. C.; Armes, S. P. *J. Am. Chem. Soc.* **1999**, *121*, 4288.

(25) Lee, A. S.; Gast, A. P.; Buthun, V.; Armes, S. P. *Macromolecules* **1999**, *32*, 4302.

(26) Wooley, K. L. *J. Polym. Sci.* **2000**, *38*, 1397.

(27) Kwong, G. S.; Naito, M.; Yokoyama, M.; Okano, T.; Sakuray, Y.; Kataoka, K. *Pharm. Res.* **1995**,*12*, 92.

(28) Kataoka, K.; Kwong, G. S.; Yokoyama, M.; Okano, T.; Sakurai, Y. *J. Controlled Release* **1993**, *24*, 119.

(29) Harada, A.; Kataoka, K. *Macromolecules* **1995**, *28*, 5294.

(30) Kataoka, K.; Harashima, H. *Adv. Drug Delivery Rev.* **2001**, *52*, 151.

(31) Yamamoto, Y.; Nagasaki, Y.; Kato, Y.; Sugiyama, Y.; Kataoka K. *J. Controlled Release* **2001**, *77*, 27.

(32) Nagasaki, Y.; Yasugi, K.; Yamamoto, Y.; Harada, A.; Kataoka, K. *Biomacromolecules* **2001**, *2*, 1067.

(33) Munk, P.; Procházka, K.; Tuzar, Z.; Webber, S. E. *CHEMTECH* **1998**, *28* (10), 20.

(34) Kiserow, D.; Procházka, K.; Ramireddy, C.; Tuzar, Z.; Munk, P.; Webber, S. E. *Macromolecules* **1992**, *25*, 461.

(35) Procházka, K.; Kiserow, D.; Ramireddy, C.; Tuzar, Z.; Munk, P.; Webber, S. E. *Macromolecules* **1992**, *25*, 454.

(36) Tuzar, Z.; Kratochvíl, P.; Procházka, K.; Munk, P. *Collect. Czech. Chem. Commun.* **1993**, *58*, 2362.

(37) Ramireddy, C.; Tuzar, Z.; Procházka, K.; Webber, S. E.; Munk, P. *Macromolecule*s **1992**, *25*, 2541.

(38) Tuzar, Z.; Procházka, K.; Zusková, I.; Munk, P. *Polym. Prepr.* **1993**, *34* (1), 1038.

(39) Tian, M.; Quin, A.; Ramireddy, C.; Webber, S. E.; Munk, P.; Tuzar, Z.; Procházka, K. *Langmuir* **1993**, *9*, 1741.

(40) Teng, Y.; Morrison, M.; Munk, P.; Webber, S. E.; Procházka, K. *Macromolecules* **1998**, *31*, 3578.

(41) Štěpánek, M.; Krijtová, K.; Limpouchová, Z.; Procházka, K.; Teng, Y.; Webber, S. E.; Munk, P. *Acta Polym.* **1998**, *49*, 96; **1998**, *49*, 103.

(42) Procházka, K.; Martin, T. J.; Munk, P.; Webber, S. E. *Macromolecules* **1996**, *29*, 6518.

(43) Štěpánek, M.; Procházka, K. *Langmuir* **1999**, *15*, 8800.

(44) Štěpánek, M.; Procházka, K.; Brown, W. *Langmuir* **2000**, *16*, 2502.

(45) Karymov, M. A.; Procházka, K.; Mendenhall, J. M.; Martin, T. J.; Munk, P.; Webber, S. E. *Langmuir* **1996**, *12*, 748.

(46) Štěpánek, M.; Krijtová, K.; Procházka, K.; Teng, Y.; Webber, S. E. *Colloids and Surf., A* **1999**, *147*, 79.

(47) Štěpánek, M.; Podhájecká, K.; Tesařová, E.; Procházka, K.; Tuzar, Z.; Brown, W. *Langmuir* **2001**, *17*, 4240.

(48) Štěpánek, M.; Podhájecká, K.; Procházka, K.; Brown, W. *Langmuir* **2001**, *17*, 4245.

(49) Matějíček, P.; Limpouchová, Z.; Uhlík, F.; Procházka, K.; Tuzar, Z.; Webber, S. E. *Collect. Czech. Chem. Commun.* **2002**, *67*, 531.

(50) Uhlík, F.; Limpouchová, Z.; Matějíček, P.; Procházka, K.; Tuzar, Z.; Webber, S. E. *Macromolecules* **2002**, *35*, 9497.

(51) Matějíček, P.; Uhlík, F.; Limpouchová, Z.; Procházka, K.; Tuzar, Z.; Webber, S. E. *Macromolecules* **2002**, *35*, 9487.

(52) Uhlík, F.; Limpouchová, Z.; Procházka, K. *J. Chem. Phys.*, in press.

(53) Pincus, P. *Macromolecules* **1991**, *24*, 2912.

(54) Israels, R.; Leermakers, F. A. M.; Fleer, G. J.; Zhulina, E. B. *Macromolecules* **1994**, *27*, 3249.

(55) Borisov, O. V.; Zhulina, E. B.; Birstein, T. M. *Macromolecules* **1994**, *27*, 4795.

(56) Lyatskaya, Yu. V.; Leermakers, F. M. A.; Fleer, G. J.; Zhulina, E. B.; Birstein, T. M. *Macromolecules* **1995**, *28*, 3562.

(57) Wijmans, C. M.; Zhulina, E. B.; Fleer, G. J. *Macromolecules* **1994**, *27*, 3238.
(58) Shusharina, N. P.; Nyrkova, I. A.; Khokhlov, A. R. *Macromolecules* **1996**, *29*, 3167.
(59) Shusharina, N. P.; Linse, P.; Khokhlov, A. R. *Macromolecules* **2000**, *33*, 3829.
(60) Misra, S.; Mattice, W. L.; Napper, D. H. *Macromolecules* **1994**, *27*, 7090.
(61) Groenewegen, W.; Ugelhaaf, S. U.; Lapp, A.; van der Maarel, J. R. C. *Macromolecules* **2000**, *33*, 3283.
(62) Katchalski, A. *J. Polym. Sci.* **1951**, *7*, 393.
(63) Arnold, R. *J. Colloid Sci.* **1957**, *1*, 549.
(64) Anufrieva, E. V.; Birshtein, T. M.; Nekrasova, T. N.; Ptitsyn, C. B.; Scheveleva, T. V. *J. Polym. Sci., Part C* **1968**, *16*, 3519.
(65) Delben, F.; Crezcenzi, V.; Quadrifoglio, F. *Eur. Polym. J.* **1972**, *8*, 933.
(66) Koenig, J. L.; Angood, A. C.; Semen, J.; Lando, J. B. *J. Am. Chem. Soc.* **1969**, *91*, 7250.
(67) Ghiggino, K. P.; Tan, K. L. In *Polymer Photophysics*; Phillips, D., Ed.; Chapman and Hall: London, 1985; Chapter 7.
(68) Wang, Y.; Morawetz, H. *Macromolecules* **1986**, *19*, 1925.
(69) Bednář, B.; Trněná, J.; Svoboda, P.; Vajda, Š.; Fidler, V.; Procházka, K. *Macromolecules* **1991**, *24*, 2054.
(70) Soutar, I.; Swanson, L. *Macromolecules* **1994**, *27*, 4304.
(71) Förster, S.; Hermsdorf, N.; Bottcher, C.; Lindner, P. *Macromolecules* **2002**, *35*, 4096.
(72) Förster, T. *Discuss. Faraday Soc.* **1959**, *7*, 27.
(73) Berleman, I. B. *Energy Transfer Parameters of Aromatic Compounds*; Academic Press: New York, London, 1973.
(74) Holden, D. A.; Guillet, J. E. *Macromolecules* **1980**, *13*, 289.
(75) Liu, G.; Guillet, J. E.; Al-Takrity, T. B.; Jenkins, A. D.; Walton, D. R. M. *Macromolecules* **1991**, *24*, 68.
(76) Martin, T. J.; Webber, S. E. *Macromolecules* **1995**, *28*, 8845.
(77) Morawetz, H. *J. Lumin.* **1989**, *43*, 59.
(78) Jakeš, J. *Czech. J. Phys.* **1988**, *B38*, 1305.
(79) Bekiranov, S.; Bruinsma, R.; Pincus, P. *Europhys. Lett.* **1993**, *24*, 171.
(80) Zeghal, A.; Auvray, L. *Europhys. Lett.* **1999**, *45*, 482.
(81) Mathur, A. M.; Drescher, B.; Scranton, A. B.; Klier, J. *Nature* **1998**, *392*, 367.
(82) Iliopoulos, I.; Audebert, R. *Eur. Polym. J.* **1998**, *24*, 171.
(83) Schuch, H.; Klingler, J.; Rossamanith, P.; Frechen, T.; Gerst, M.; Feldthusen, J.; Müller, A. H. E. *Macromolecules* **2000**, *33*, 1734.
(84) Erhardt, R.; Böcker, A.; Zettl, H.; Kaya, H.; Pychhout-Hintzen, W.; Krausch, G.; Abetz, V.; Müller, A. H. E. *Macromolecules* **2001**, *34*, 1069.
(85) Magde, D.; Elson, E. L.; Webb, W. W. *Phys. Rev. Lett.* **1997**, *29*, 705.
(86) Webb, W. E. In *Fluorescence Correlation Spectroscopy Theory and Applications*; Riedler, R., Elson, E. S., Eds.; Springer-Verlag: Berlin, 2001.
(87) Thompson, N. L. In *Topics in Fluorescence Spectroscopy;* Lakowicz, J. R., Ed.; Plenum Press: New York, 1991; Vol. 1, Chapter 6.
(88) Hink, M. A.; van Hoek, A.; Visser, A. J. W. G. *Langmuir* **1994**, *4*, 992.
(89) Koppel, D. E. *Phys. Rev.* **1974**, *10*, 1938.
(90) Kask, P.; Günter, R.; Axhausen, P. *Eur. Biophys. J.* **1997**, *25*, 163.
(91) Meseth, U.; Wohland, T.; Rigler, R.; Vogel, H. *Biophys. J.* **1999**, *80*, 2987.
(92) Edman, L. *J. Phys. Chem. A* **2000**, *104*, 6165.
(93) Wohland, T.; Rigler, R.; Vogel, H. *Biophys. J.* **2000**, *80*, 2987.
(94) Magde, D.; Elson, E. L.; Webb, W. W. *Biopolymers* **1974**, *13*, 29.
(95) Elson, E. L.; Magde, D. *Biopolymers* **1874**, *13*, 1.
(96) Magde, D.; Webb, W. W.; Elson, E. L. *Biopolymers* **1978**, *17*, 361.
(97) Aragón, S. R.; Pecora, R. *Biopolymers* **1975**, *14*, 119.
(98) Aragón, S. R.; Pecora, R. *J. Chem. Phys.* **1976**, *64*, 1791.
(99) Hess, S. T.; Huang, S.; Heikal, A. A.; Webb, W. W. *Biochemistry* **2002**, *41*, 697.
(100) Jelínek, K.; Uhlík, F.; Limpouchová, Z.; Procházka, K. *J. Phys. Chem. B* **2003**, *107*, 8241.
(101) Humpolíčková, J.; Procházka, K.; Hof, M.; Tuzar, Z.; Špírková, M. *Langmuir* **2003**, *19*, 4111.
(102) Kratochvíl, P. *Classical Light Scattering from Polymer Solutions, Polymer Science Library 5*; Jennkins, A. D., Ed.; Elsevier: Amsterdam, 1987.
(103) Tuzar, Z.; Kratochvíl, P. *Collect. Czech. Chem. Commun.* **1967**, *32*, 3358.
(104) Hartley, P. G.; Scales, P. J. *Langmuir* **1998**, *14*, 6948.
(105) Zhmund, B. V.; Meurk, A.; Bergstrom, L. *J. Colloid Interface Sci.* **1998**, *207*, 332.
(106) Claesson, P. M.; Ninham, B. W. *Langmuir* **1992**, *8*, 1406.
(107) Briscoe, W. H.; Horn, R. G. *Langmuir* **2002**, *18*, 3945.
(108) *Polymer Handbook*; Brandrup, J., Immergut, E. H., Eds.; Interscience Publishers: New York, 1967.